Supplementary materials for this article are available at 10.1007/s13253-011-0072-8.

Multivariate Spatial Analysis of Climate Change Projections

Tamara A. GREASBY and Stephan R. SAIN

The goal of this work is to characterize the annual temperature for regional climate models. Of interest for impacts studies, these profiles and the potential change in these profiles are a new way to describe climate change and the inherent uncertainty. To that end, we propose a Bayesian hierarchical spatial model to simultaneously model the temperature profile for the four seasons of the year, current and future. These profiles are then analyzed focusing on understanding how they change over time, how they vary spatially, and how they vary between five different regional climate models. The results show that for temperature, the regional models have different profile shapes depending on a number of factors including spatial location, driving climate model, and regional climate model. This article has supplementary material online.

Key Words: Hierarchical model; Intrinsic Markov random field; Regional climate models.

1. INTRODUCTION

Numerical models of the Earth's climate system are important tools for producing projections of climate change. Modern atmosphere–ocean general circulation models (GCMs) couple an atmospheric model with an ocean model and are effective at studying processes and forcings on larger spatial scales. Many climate change impacts studies, however, require projections on regional and even local spatial scales. This has driven recent interest in downscaling and approaches based on high-resolution climate models, including programs such as the North American Regional Climate Change Assessment Program (NARCCAP; Mearns et al. 2009, 2011). The recent assessment report produced by the Intergovernmental Panel on Climate Change (IPCC) contains excellent background information and a wealth of references on climate, climate change, and climate models (Solomon et al. 2007, *http://www.ipcc.ch*).

Tamara A. Greasby (✉) is a Postgraduate Scientist (E-mail: *tgreasby@ucar.edu*) and Stephan R. Sain is a Scientist, Institute for Mathematics Applied to Geosciences, National Center for Atmospheric Research, Boulder, CO, USA.

Journal of Agricultural, Biological, and Environmental Statistics, Volume 16, Number 4, Pages 571–585
DOI: 10.1007/s13253-011-0072-8

Often, statistical analysis of climate model output has focused on annual or seasonal summaries aggregated over global, hemispheric, or continental spatial scales and possibly analyzed as time series or with spatial statistical models (e.g., Tebaldi et al. 2005; Furrer et al. 2007; Berliner and Kim 2008; Smith et al. 2009; Tebaldi and Sansó 2009; Buser, Kunsch, and Weber 2010; Kaufman and Sain 2010; Sain, Nychka, and Mearns 2011 etc.). The goal of this research is somewhat different in that we seek to establish an annual profile of temperature that is allowed to vary across a spatial domain and then examine how this profile changes with the assumed anthropogenic forcings incorporated into the climate models. While changes in the seasonal summaries by themselves are important indicators of climate change, many impacts researchers, for example, those interested in hydrology, agriculture, or public health, are interested in changes that may span several seasons, and further understanding of potential changes to seasonality is also important (e.g., is what we think of as "summer" not only getting warmer but also getting longer?). Further, by allowing these profiles and the changes to these profiles vary across space, we seek to identify regions across the domain that might be at an increased risk for climate change.

Additionally we seek to understand how these profiles vary across the different models and modeling choices used in the NARCCAP experiment. Quantifying this model-to-model uncertainty can be crucial to the development of methods for combining the output across a multimodel ensemble (e.g., to be used for further analysis and in conjunction with impacts studies), to the development of future regional climate modeling experiments, and to the further understanding of how the different models capture the physics that determine the Earth's climate.

With these goals in mind, this paper represents an initial approach to establishing this profile through a multivariate spatial statistical model that links the four (winter, spring, summer, fall) seasonal summaries. While this approach does not allow us to address more complex questions such as of the length of summer, it is a first step toward understanding the interactions between climate model and seasonality as well as understanding the uncertainty related to climate model choice. Further, it can be expanded to include more complex statistical formulations that have the flexibility to better understand characteristics such as changing seasonality.

1.1. GLOBAL CLIMATE MODELS, REGIONAL CLIMATE MODELS, AND UNCERTAINTY

GCMs are large-scale, computationally demanding numerical models based on scientists' current understanding of the Earth's climate system and the flows of water, energy, gas, etc. between and within the various components (e.g., atmosphere, oceans, cryosphere, biosphere, etc.) of the climate system. When modeling future climate, GCMs also attempt to incorporate changes in the forcings that influence the climate system. Of particular importance are changes in greenhouse gasses and other anthropogenic or human-related factors that influence the Earth's climate.

An important aspect when considering any projection of future climate is understanding the uncertainties associated with such projections. Generally speaking, there are three main sources of uncertainty (see, for example, the commentary in Mearns 2010, and the references therein). The first is uncertainty about future greenhouse gas and aerosol emissions, and a variety of emissions scenarios have been considered. Of course it is not clear which or even if a predefined scenario will occur. Another source of uncertainty is the climate system's response to changing emissions, and, finally, the natural variability of the climate system must also be considered. When climate models are added to the mix, there are a number of additional uncertainties that arise. For example, there is uncertainty from the different assumptions about physical processes and how they are implemented in climate models (an example of a type of structural uncertainty) as well as uncertainties that arise from how sub-grid-scale processes are approximated (an example of a type of parametric uncertainty). Collections of model output, termed ensembles, are often used to explore these uncertainties. These ensembles might be made up from a single model with different initial conditions or with different assumptions about physical processes (i.e., perturbed physics ensembles; see, for example, Murphy et al. 2007) or from entirely different models (i.e., multimodel ensembles; see, for example, Tebaldi and Knutti 2007).

GCMs generally have grid boxes on the order of a 100–200 kilometers, and the large computational demands of GCMs make it infeasible to run them at higher resolutions. Unfortunately, many impacts studies require climate and climate change projections on a much finer grid. Downscaling refers to methods that use the information from GCMs to model climate at higher resolutions. Statistical downscaling uses empirical relationships between GCM output and observations at regional and local levels. One challenge to this approach is the implicit assumption that the empirical relationship will remain the same in the future. Dynamic downscaling is an alternative that uses higher-resolution climate models. However, there is generally some price to be paid for the increase in resolution. For example, one approach simply uses the atmospheric component of a fully coupled GCM with observed or perturbed sea-surface temperatures in place of an ocean model.

Another approach to downscaling involves regional climate models (RCMs), which have grid boxes on the order 25–50 kilometers. Typically run over a limited spatial domain, RCMs use time-dependent boundary conditions such as temperature, winds, atmospheric moisture, etc. supplied by a global climate model. Downscaling and the choice of climate model resolution introduces another source of uncertainty in projections of future climate. NARCCAP has the goal of exploring these uncertainties in climate change projections by creating an ensemble of RCM output using a different combinations of GCMs and RCMs in a statistically designed experiment.

1.2. MODEL OUTPUT

For this paper, seasonal averages were created for five different RCMs from the NARCCAP experiment. Three of the RCMs are both driven by the same global model, NCAR's Community Climate System Model (CCSM) to achieve some control over that source of uncertainty. The remaining two models were driven by Canada's Coupled Global Climate Model (CGCM3). The three regional models driven by CCSM are the Canadian Regional Climate Model (CRCM), the Weather Research and Forecasting model (WRFG), and the PSU/NCAR mesoscale model (MM5I). WRFG and CRCM models driven by the CGCM3 model were also used. The current run of each RCM spans 1970–2000 while the future run spans 2040–2070. The future run also uses the A2 emissions scenario (Nakicenovic et al. 2000) which increases CO_2 concentration levels from the current values of around 380 ppm to about 870 ppm by the end of the 21st century.

For temperature, average values were computed for each season for all years in which the model results are available. The seasons are defined as follows: winter (December, January, February), spring (March, April, May), summer (June, July, August), and fall (September, October, November). The average for each RCM was computed separately.

1.3. PAPER OUTLINE

In the following section, we outline a multivariate spatial statistical model for annual profiles constructed from seasonal summaries of climate model output. Section 3 discusses some results, based on a subset of the NARCCAP ensemble (at this point in time, the output from the entire NARCCAP experiment is not available), focusing on understanding how these profiles change over time, how they vary spatially, and how they vary between two different RCMs. Finally, Section 4 discusses some extensions and plans for future work.

2. A BAYESIAN HIERARCHICAL SPATIAL MODEL

With a multivariate spatial model based on an intrinsic Markov random field at its core, we develop a Bayesian hierarchical statistical model (Banerjee, Carlin, and Gelfand 2004; Rue and Held 2005) for the annual profiles and to aid in modeling the uncertainty about those profiles. The statistical model consists of three levels: data, process, and prior, and Markov chain Monte Carlo (MCMC; e.g., Gilks, Richardson, and Spiegelhalter 1996) via a Gibbs sampler (Geman and Geman 1984; Gelfand and Smith 1990; Gelfand et al. 1990) is used to sample from the posterior distribution of the model parameters.

Throughout this paper, the following notation will be used. Let Y be an $8N \times 1$ vector representing seasonal average temperature, where N is the number of grid boxes. There are eight values at each grid box representing the four seasons for each of two runs (current and future) of the regional model representing. Y is structured as follows:

$$Y = \left[Y_{cw1}^T \dots Y_{cwN}^T \quad Y_{csp1}^T \dots Y_{cs1}^T \dots Y_{cN}^T \quad Y_{fw1}^T\right],$$

where c or f represents current or future, w, sp, s, and f represent the four seasons, and $1, \dots, N$ represents the grid-box number.

2.1. DATA LEVEL

The following statistical model is used for temperature:

$$Y = X\beta + U + \varepsilon, \tag{2.1}$$

where X is a regression matrix with dimension $8N \times 18$. Main effects are considered for the four seasons, run (current and future), elevation, and a land–sea indicator. Also, two way interactions are considered between all variables, with the exception of elevation and the land–sea indicator.

Other predictors such as soil moisture (an input to regional climate models), latitude and longitude, and three-way interactions were considered but did not improve model fit. The $8N \times 1$ vector U is a spatial effect, and the $8N \times 1$ error vector, ε, is assumed to be independently and identically Gaussian distributed. With these assumptions, Y is distributed as follows:

$$Y|U, \beta, \sigma^2 \sim N(X\beta + U, \sigma^2 I_{8N}).$$

2.2. PROCESS LEVEL

The spatial component of (2.1) is specified at the process level. Consider the vector $U = [U_1^T \ U_2^T \ \ldots \ U_8^T]'$ where all U_i are vectors of length N representing a random spatial field for each season from the current and future runs of the regional climate model. Care needs to be taken in considering the spatial covariance of U. There are 14,606 and 16,100 grid boxes in the WRFG and CRCM models, respectively, which make many specifications based, for example, on geostatistical ideas challenging. That, along with the fact that the climate models are generally on regular spatial grids and that the scope of any inference is also on that same regular grid, we assume that each U_i follows a first-order, intrinsic Gaussian Markov random field (IGMRF; see Rue and Held 2005, Chapter 3) with mean 0 and precision matrix V. Further, when all eight U_i are modeled jointly, a separable form is assumed, i.e., $[U] \propto |S|^{N/2}\exp(-\frac{1}{2}(U^T(S \otimes V)U))$, where S is 8×8, and V is $N \times N$. For identifiability, the constraint $\sum_{j=1}^{N} U_{ij} = 0$ is placed on the U_i's. A similar construction was utilized in Cooley and Sain (2010) for the analysis of precipitation extremes from RCMs. Note that S is 8×8 allowing for correlation between the 8 random effects, 4 for each season, current and future.

It should be noted that IGMRFs are improper, but are well suited for prior distributions. To construct the precision matrix, the diagonal entries of V, v_{ii}, are the number of neighbors of the ith grid box. The off-diagonal elements, v_{ij} take the value -1 when grid boxes i and j are neighbors. Otherwise, they are 0. (In this case, "neighbors" are defined to be the grid boxes directly north, south, east, and west of the grid box of interest.) So, not only are we specifying the precision matrix rather than the covariance matrix to keep from having to perform expensive matrix inversions, the precision matrix is sparse, and sparse-matrix methods can be used for additional computation advantages (Furrer and Sain 2010).

Finally, it is clear from this formulation that all rows and columns of V sum to 0. Thus V is rank-deficient, having rank of $N - 1$. One advantage to the first-order IGMRFs is that they are invariant to the addition of a constant.

2.3. PRIOR LEVEL

Prior distributions for β, σ^2, and S^{-1} must also be specified.

First, β is assumed to be normally distributed with mean μ and covariance Σ. The element of μ corresponding to the intercept is estimated by the mean temperature, and remaining values are set to 0. The covariance of β is assumed to be diagonal. Various choices for μ and Σ were considered with the goal of choosing values that were not overly informative. Initial tests showed that specific choices had little impact on the posterior.

Noninformative priors are also used for both σ^2 and S^{-1}. Specifically, σ^2 is assumed to be inversely proportional to itself, while S^{-1} is proportional to $|S|^{\frac{8-1}{2}}$.

2.4. MODEL FITTING

Sampling a multivariate posterior distribution with a Gibbs sampler involves drawing repeated samples from the conditional distributions of the statistical model parameters (conditional on the data and current values of other model parameters). These conditional distributions are given in the Appendix. A variety of starting values were used to initialize the chains, and convergence was monitored via trace plots as well as using Gelman's $\sqrt{R}$ statistic, which measures consistency across the chains (Gelman 1996). Chains of length 8500 were run, with the first 1000 taken as the burn-in. Following burn-in, every 13th sample was retained for posterior inference.

Residuals based on comparing the posterior mean of $X\beta + U$ from (2.1) were examined, as well as other diagnostics used to ensure model adequacy. Plots of residuals do not show any strong, systematic spatial patterns indicating that this statistical model adequately captures the spatial dependence in the climate model output.

3. RESULTS

Our aim is to analyze the annual profile of temperature to see how this profile changes between the current and future runs of the regional climate models, in effect seeing how this profile changes in light of the anthropogenic forcings included in the future run. We will also examine how these changes vary spatially and between climate models. Of particular interest is the concept of interactions—we want to investigate the impacts of RCM, the boundary conditions from the GCM, the greenhouse gas forcings, the season, and possible regional differences. For example, one might believe that two RCMs, run with the same boundary conditions and forcings, would lead to similar temperature profiles. In another level of complexity, a profile may be shifted up or down relative to the other, indicating that one model simply runs hotter than another, regardless of season or forcing. This would be indicative of a strong RCM or greenhouse gas affect effect, but little or no interaction between RCM, forcing, or season.

One might expect the temperature for a given season to depend on the RCM. For example, the winter season for one model might be hotter than the rest, while the summer season for that same model is colder than the rest. This would suggest an interaction between RCM and season. When the boundary conditions supplied by the GCM are also varied, even more complex interactions are possible. Further, understanding and quantifying the magnitude of these effects would suggest how to design future experiments (i.e., more or less RCMs, more or less GCMs, different combinations of RCM and GCM, etc.) or even how to consider combining results from multimodel experiments and integrating these results into impacts studies. Understanding the response of an RCM to a particular GCM and the connection between the physics implemented in the two models would give modelers insight into how to improve their models.

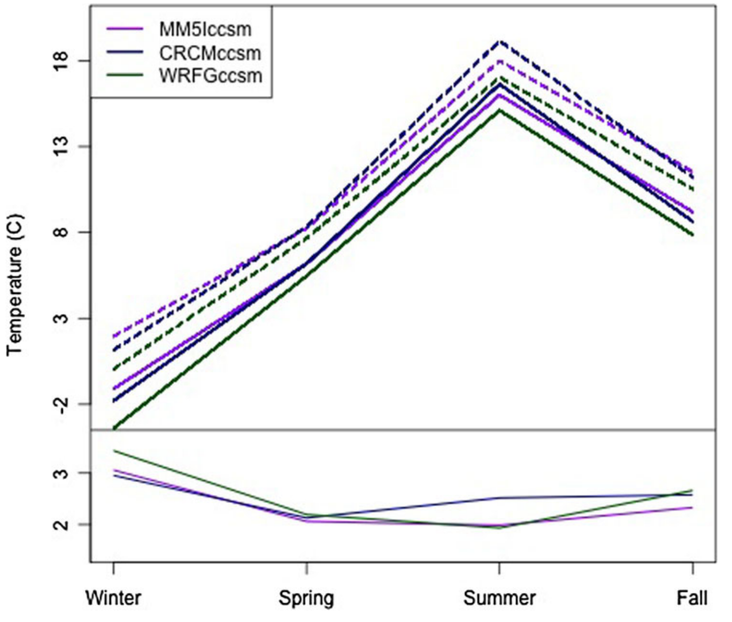

Figure 1. Temperature profiles for the current (solid) and future (dashed) time periods in degrees Celsius. The projected differences (future minus current) are shown below the horizontal gray line. Credible intervals in this case are quite small and are not visible in this figure. All three RCMs shown were forced by the CCSM CGM.

The results from our analysis will be broken into two sections. In the first, the results from three RCMs driven by the same GCM will be investigated with the intention of looking at the response of different regional climate models to the same boundary conditions from the GCM and greenhouse gas forcings. In the second, the results from runs with two RCMs and two GCMs will be investigated. In both of these, the statistical analysis is done for each run of the RCM separately, making the comparisons more qualitative.

3.1. RCM RESPONSE TO A COMMON DRIVING MODEL

Figure 1 shows the overall temperature profiles for the current and future years and the projected changes across the domain for each of the seasons. The three models shown here are all driven by the CCSM global model. We note some of the more dramatic features suggested by Figure 1:

- All models experience the greatest temperature change in winter.
- Two models, the MM5I and the WRFG, have the smallest change in summer, while CRCM has the smallest change in spring.
- The WRFG model has the coolest temperatures for current/future relative to the other two models.
- The CRCM model has the hottest temperatures in spring and summer. The MM5I model is hotter in the fall and winter.

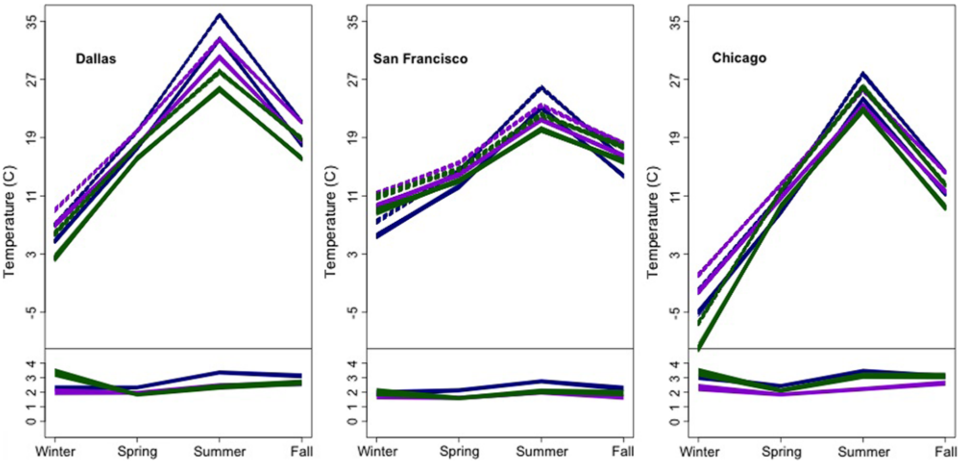

Figure 2. Current, future, and temperature change profiles in degrees Celsius for three metropolitan areas. The shaded bands indicate the 90% credible interval. The blue curves represent the CRCMccsm model, the purple curve the MM5Iccsm model, and the green curve the WRFGccsm model. The posterior mean difference was computed by averaging all grid boxes contained in the metropolitan area, as defined by the US Census Bureau.

This indicates that temperature profile and temperature change profile depend on many factors, not simply additive effects from RCM or forcing. First, the response of the RCMs to the boundary conditions supplied by the GCM and the forcing from the changing greenhouse gasses is not the same for all regional models. Second, the response is not consistent across seasons for all RCMs. While a more comprehensive analysis is beyond the scope of this paper, these results suggest that there is evidence for the presence of interactions between RCM, season, and the greenhouse gas forcing and further suggest that a more comprehensive analysis to quantify these effects and interactions is an important next step.

It is also possible to determine if there is spatial variability in these profiles. Figure 2 shows the same profiles for three specific metropolitan areas as defined in the U.S. Census as Consolidated Metropolitan Statistical Areas (CMSA). To compute these profiles, an average is computed for the metropolitan area using every thirteenth observation from each grid box contained within the region. Of note in Figure 2:

- In the average profile, winter had the largest change. In the case of San Francisco, winter does not have the largest change. In Dallas, winter has the largest change for the WRFG model, but not for the other two. In Chicago, the change in winter appears to be close to the change in summer.

- The coolest model is not consistent across all regions. In Dallas, the WRFG model is the coolest across all seasons. In San Francisco, the WRFG model is coolest in the summer, but not in any other season. Likewise, the hottest model is not consistent across all regions. In summer, the CRCM model is the hottest for Sallas and San Francisco.

- For Dallas and San Francisco, the credible intervals for temperature change for WRFG and MM5I overlap for at least three seasons. In Chicago however, the credible

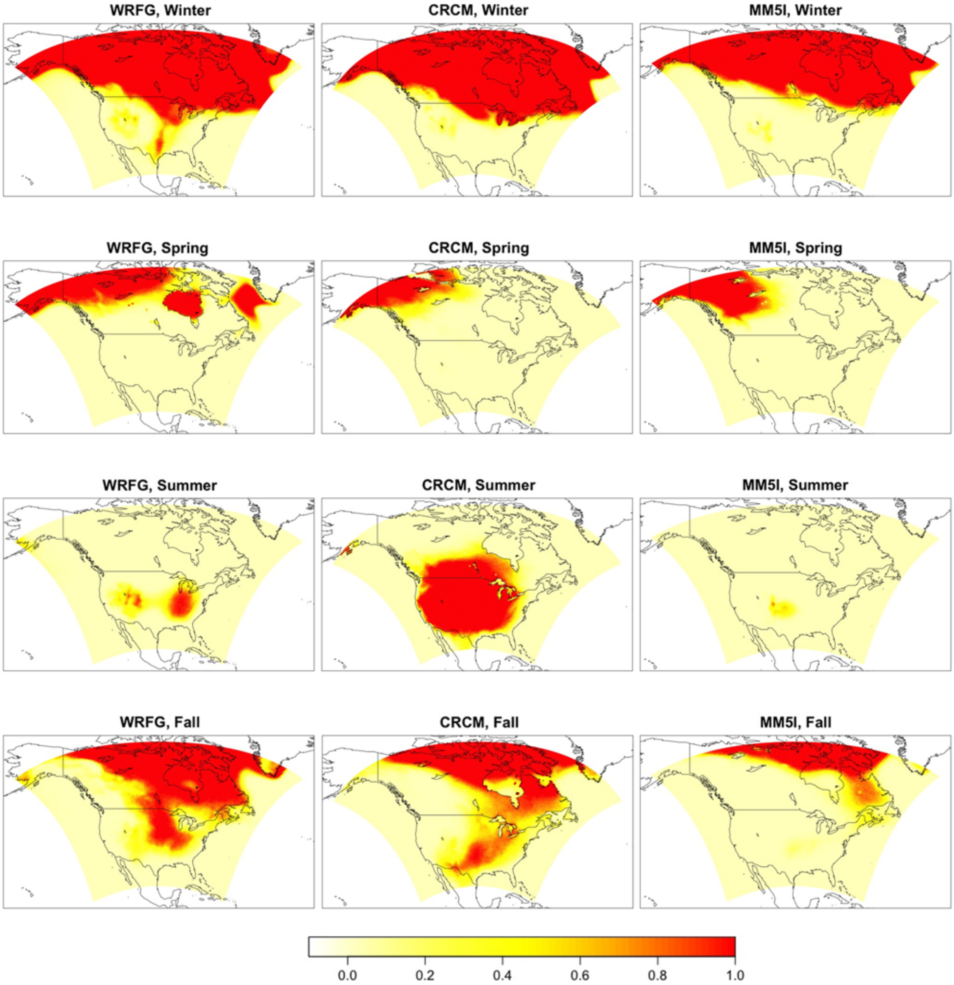

Figure 3. Posterior probability of experiencing a change in temperature greater than 3 degrees Celsius for each grid box and each season (winter, spring, summer, and fall). Each of these models was driven by the CCSM model.

intervals overlap for the WRFG and CCSM models. The MM5I change looks quite different.

These plots suggest temperature profiles, and their change are subject to differences based on the regional climate model, the region, and the season. Moreover, it suggests that there are interactions between all these factors, stressing the importance to consider the spatial variability, in particular for impacts studies on regional and local scales.

Figure 3 shows the estimated probability of a temperature increase of more than 3 degrees Celsius for the CRCM, WRFG, and MM5i models driven by CCSM for each of the four seasons. These plots highlights the major difference between climate models shown in the previous plot. In winter, all models agree that the larger increases in temperature occur in the northern latitudes. During the summer, the CRCM model shows larger increases in the continental United States than the WRFG and MM5I models. The MM5I model shows hardly any change. Thus the pattern seen in the profiles for the metropolitan areas are present throughout the continental United States, with the exception of the Southeast and Eastern coasts. In spring, all models highlight change in Alaska and Northwestern Canada. The WRFG model shows larger increases in the Hudson Bay and the Northwestern passages that is not apparent in the other two. In the fall, all models show increases occurring along the northern border of the domain. These increases stretch down through eastern Canada, through the midwestern United States and into the four-corners area for the CRCM and WRFG models. In the WRFG model, however, the increases extend more to the south, into Mexico.

These plots indicate that no region or area is necessarily vulnerable to large temperature increases across all seasons. While there appears to be small change in the southern part of the domain that is consistent across all seasons, the increases as one moves north is both region and model dependent. It does appear that the northernmost section of the domain is most vulnerable to change in winter, spring, and fall, while the more central regions are vulnerable to larger change in the summer and fall.

Finally, we note that the effects of other covariates included in the data model are as expected and are mostly consistent across climate model. Elevation has a negative relationship with temperature, and the magnitude of that effect is comparable for all models. Land temperatures are on average lower than the ones at sea. The WRFG and MM5I models shows less of a land/sea effect than the CRCM model. Another effect of interest is the interaction between run, current and future, and elevation. Overall this effect is significant for CRCM and WRFG but small, less than –0.2 Celsius. This indicates higher elevations are less subject to climate change than lower elevations. The interaction between run and land and sea is not significant for the CRCM or MM5I models and is also small, less than -0.2 for the WRFG model. Information about the posteriors of the S matrices can be found in the online supplement.

3.2. RCM–GCM INTERACTIONS

The previous section showed the profile variability experienced when the boundary conditions were provided from the same GCM and greenhouse gas forcings were the same for current and future runs of each RCM. In this section, we will investigate the role of the previously mentioned factors when the boundary conditions are varied. Figure 4 shows the average estimated profiles and change for the CRCM and WRFG models driven by both the CCSM and CGCM3 models. Note that:

- The two models driven by the CGCM3 model have similarly shaped temperature change profiles. This is not true for the CCSM models.
- The CGCM3 models indicate an interaction between the regional model and the season—the WRFG model is hotter in winter and spring and cooler in summer. For the CCSM driven models, the WRFG model is cooler than the CRCM model across all seasons.

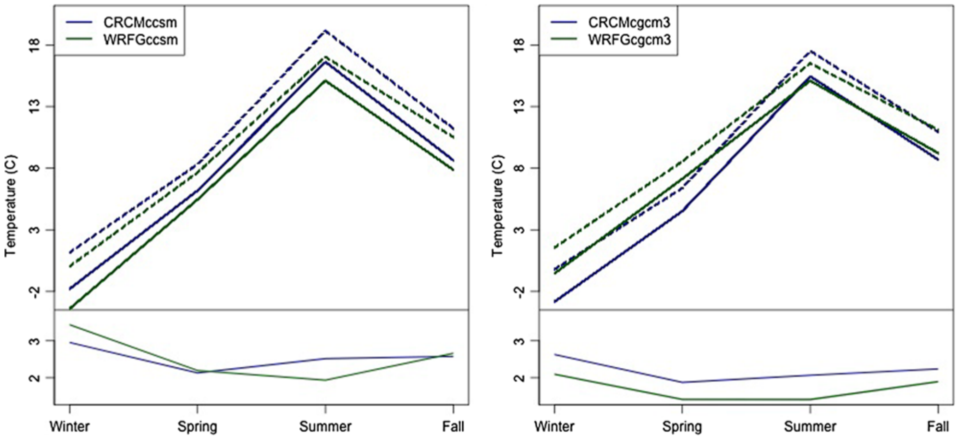

Figure 4. Temperature profiles for the current (solid) and future (dashed) time periods and projected difference in degrees Celsius. The shaded bands indicate the 90% credible intervals. The models in the left plot were driven by the CGCM3 model, while those on the right were driven by the CCSM model.

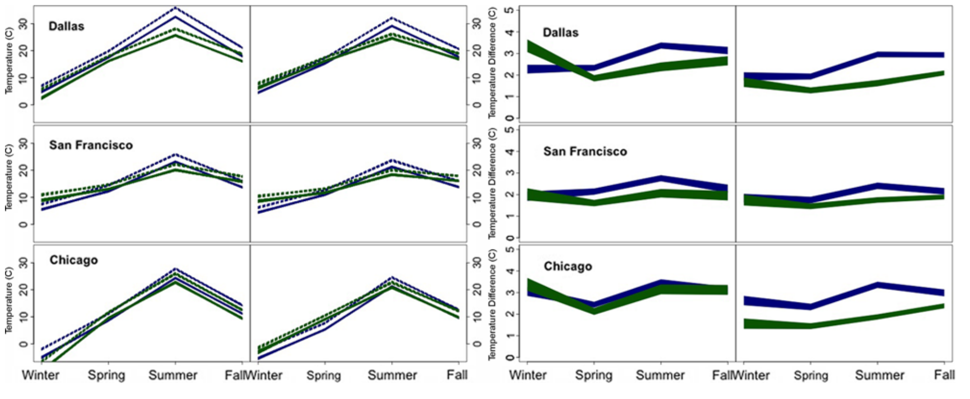

Figure 5. Plots on the right show current and future temperature profiles in degrees Celsius for 3 metropolitan areas. The projected temperature change is shown in the plots on the left. The shaded bands indicate the 90% credible interval. The blue curves represent the CRCM regional model, and the green curve the WRFG regional model. Plots in the first column are from the CCSM model, while plots in the second column are from the CGCM3 model.

- In summer, the CRCM CCSM future values are within a degree of the current WRFG values. For the CGCM3 driven models though, the future CCSM values are closer to the WRFG future values than the WRFG current values.

The temperature profiles and changes for each of the previously mentioned regions are shown in Figure 5. These profiles show substantial spatial variation. Particularly of note,

- The profile shapes appear to be consistent within a city for the same RCM when driven by these two GCMs. They do differ in magnitude however.
- In Dallas the CRCM model is hotter than WRFG when driven by both the CCSM and CGCM3 models. In San Francisco, the CRCM model is hotter than the WRFG

in winter and fall for both GCMs. In Chicago, the hotter model in winter depends on the GCM.

- Overall, Chicago looks most like the average profile shown in Figure 4. The other two cities show a clear level difference in temperature.
- The similar change profile plots from the overall average for the CGCM3 model is not repeated in any of these metropolitan areas.
- With the CGCM3 forcings, the CRCM model always has the highest projected change (or the same). With CCSM, the model with the largest projected change depends on the season.
- In Chicago, the credible intervals for projected change when driven by CCSM overlap for all seasons. When driven by CGCM3, none of the credible intervals overlap.

As in the previous section, these results suggest the presence of interactions with RCM, season, location, and GCM. The presence of these interactions suggest the need for more careful analysis to quantify the magnitude of these effects, and this is the focus of much of our current research. It is interesting to note that the CGCM3 driven models show fewer RCM spatial effects than the CCSM driven models. This clearly points to the need for an analysis including more GCMs.

4. DISCUSSION, CONCLUSIONS, AND FUTURE WORK

This work introduces a novel approach to assessing climate change on the basis of climate model experiments by considering an annual profile, in this case constructed from seasonal temperature, and how that annual profile changes in response to the assumed anthropogenic forcings. At the heart of this approach is a hierarchical Bayesian construction with a multivariate spatial model to deal with spatial correlation in the climate model output. This statistical model allows quantification of the uncertainty in the changes to these annual profiles, along with the ability to examine how these profiles and changes to these profiles vary across season, space, RCM, and GCM.

This analysis specifically looks at an the annual profile change for temperature. Based on this, a relationship is shown between the three regional climate models, CRCM, WRFG (driven by the CCSM and CGCM3 global models), and MM5I (driven by the CCSM global model). These models showed substantial variability across season, across the spatial domain, and based on the regional-global model combination.

These profiles also showed that for temperature, there are no specific regions at greater risk for change across all seasons, although the north is more vulnerable for three of the seasons. It should be noted that this approach could easily be adapted to examine precipitation or any of the other climatological fields produced by these regional models; nor is it restricted regional models as ensembles of global models could be analyzed in this manner.

This work just begins to touch on the questions of interest related to the annual cycle of temperature and climate change. The presence of interactions between factors such as season, regional model, and global model shows that comparing climate models is tricky business and that a more in-depth, deliberate, and comprehensive analysis is needed. Our ultimate goal is a comprehensive statistical model for this annual cycle that spans key sources of uncertainty including the interannual variability and the variability across different models. Improved understanding of how this annual profile changes in response to anthropogenic forcings can be invaluable for impacts studies. This statistical model will continue to build on the early work of Tebaldi et al. (2005) and more recent effects in functional analysis of variance (e.g., Kaufman and Sain 2010; Sain, Nychka, and Mearns 2011). Further, the multivariate approach can be expanded to include simultaneous analysis of temperature and other covariates such as precipitation, greatly expanding on previous work in this area (e.g., Tebaldi and Sansó 2009; Sain, Furrer, and Cressie 2011).

APPENDIX

The posterior has the following form:

$$
\begin{aligned}
U, \beta, \sigma^2, S|Y \propto |(\sigma^2 \mathrm{I})|^{-\frac{1}{2}} \exp\left[-\frac{1}{2\sigma^2}(Y - X\beta - U)^T (Y - X\beta - U)\right] \\
\times |S|^{\frac{N}{2}} \exp\left[-\frac{1}{2}\left(U^T (S \otimes V) U\right)\right] \\
\times \exp\left[-\frac{1}{2}(\beta - \mu)^T \Sigma^{-1} (\beta - \mu)\right] (\sigma^2)^{-1} |S|^{\frac{8-1}{2}}.
\end{aligned}
$$

From this expression the following conditional distributions can be derived and represent the distributions that are sampled with the Gibbs sampler:

$$
\begin{aligned}
&\sigma^2|Y, U, \beta, S \propto \Gamma^{-1}\left(\frac{8N}{2}, \frac{1}{2}(Y - X\beta - U)^T (Y - X\beta - U)\right), \\
&\beta|Y, U, S, \sigma^2 \\
&\quad \propto N\left(\left(\Sigma^{-1} + \frac{X^T X}{\sigma^2}\right)^{-1} \left(\Sigma^{-1}\mu + \frac{X^T Y}{\sigma^2} - \frac{X^T U}{\sigma^2}\right), \left(\Sigma^{-1} + \frac{X^T X}{\sigma^2}\right)^{-1}\right), \\
&U_i|Y, U_{-i}, \beta S, \sigma^2 \\
&\quad \propto N\left(\left(s_{ii} V + \frac{I_N}{\sigma^2}\right)^{-1} \left(\frac{Y}{\sigma^2} - \frac{X_i \beta}{\sigma^2} - V \sum_{j \neq i} s_{ij} U_j\right), \left(s_{ii} V + \frac{I_N}{\sigma^2}\right)^{-1}\right), \\
&S|Y, U, \beta, \sigma^2 \propto W\left(N + 2(8) - 1, U^{*T} V U^*\right),
\end{aligned}
$$

where Γ^{-1} indicated the inverse gamma distribution, W the Wishart distribution, and N the Normal distribution. Further, U_{-i} indicates the collection of the elements of U except the ith, and U^* indicates the $N \times 8$ matrix with ith columns U_i.

SUPPLEMENTARY MATERIALS

Information about the posteriors of the S matrices.

ACKNOWLEDGEMENTS

This research was supported, in part, by National Science Foundation (NSF) grants ATM-0502977, ATM-0534173, and DMS-0707069, a grant from NASA ROSES (09-IDS09-34), as well as the Weather and Climate Impact Assessment Science Program at the National Center for Atmospheric Research (NCAR). NARCCAP is funded by the NSF, the U.S. Department of Energy (DoE), the National Oceanic and Atmospheric Administration (NOAA), and the U.S. Environmental Protection Agency Office of Research and Development (EPA). NCAR is managed by the University Corporation for Atmospheric Research under the sponsorship of the National Science Foundation.

[Published Online November 2011.]

REFERENCES

Banerjee, S., Carlin, B. P., and Gelfand, A. E. (2004), *Hierarchical Modeling and Analysis for Spatial Data*, Bacon Raton: Chapman & Hall/CRC Press.

Berliner, L. M., and Kim, Y. (2008), "Bayesian Design and Analysis for Superensemble Based Climate Forecasting," *Journal of Climate*, 21, 1891–1910.

Buser, C., Kunsch, H., and Weber, A. (2010), "Biases and Uncertainty in Climate Projections," *Scandinavian Journal of Statistics*, 37, 17–199.

Cooley, D., and Sain, S. R. (2010), "Spatial Hierarchical Modeling of Precipitation Extremes from a Regional Climate Model," *Journal of Agricultural, Biological, and Environmental Statistics*, 15, 381–402. doi:*10.1007/s13253-010-0023-9*.

Furrer, R., and Sain, S. R. (2010), "Spam: A Sparse Matrix R Package with Emphasis on MCMC Methods for Gaussian Markov Random Fields," *Journal of Statistical Software*, 36 (10), 1–25. ISSN:1548-7660. *http://www.jstatsoft.org/v36/i10*.

Furrer, R., Sain, S. R., Nychka, D., and Meehl, G. A. (2007), "Multivariate Bayesian Analysis of Atmosphere-Ocean General Circulation Models," *Environmental and Ecological Statistics*, 14, 249–266.

Gelfand, A. E., Hills, S. E., Racine-Poon, A., and Smith, A. F. M. (1990), "Illustration of Bayesian Inference in Normal Data Models Using Gibbs Sampling," *Journal of the American Statistical Association*, 85, 972–985.

Gelfand, A. E., and Smith, A. F. M. (1990), "Sampling-Based Approaches to Calculating Marginal Densities," *Journal of the American Statistical Association*, 85, 398–409.

Gelman, A. (1996), "Inference and Monitoring Convergence," in *Markov Chain Monte Carlo in Practice*, London: Chapman & Hall, pp. 131–144.

Geman, S., and Geman, D. (1984), "Stochastic Relaxation, Gibbs Distributions and the Bayesian Restoration of Images," *IEEE Transactions on Pattern Analysis and Machine Intelligence*, 6, 721–741.

Gilks, W. R., Richardson, S., and Spiegelhalter, D. J. (1996), "Introducing Markov Chain Monte Carlo," in *Markov Chain Monte Carlo in Practice*, London: Chapman & Hall, pp. 1–19.

Kaufman, C. G., and Sain, S. R. (2010), "Bayesian Functional ANOVA Modeling Using Gaussian Process Prior Distributions," *Bayesian Analysis*, 5, 123–150.

Mearns, L. (2010), "The Drama of Uncertainty," *Climatic Change*, 100, 77–85. ISSN:0165-0009, doi:*10.1007/s10584-010-9841-6*.

Mearns, L., Arritt, R., Biner, S., Bukovsky, M., McGinnis, S., Sain, S., Caya, D., Correia, J., Flory, D., Gutowski, W., Takle, E., Jones, R., Leung, R., Moufouma-Okia, W., McDaniel, L., Nunes, A., Qian, Y., Roads, J., Sloan, L., and Snyder, M. (2011), "The North American Regional Climate Change Assessment Program: Overview of Phase I Results," *Bulletin of the American Meteorological Society*, submitted.

Mearns, L. O., Gutowski, W., Jones, R., Leung, R., McGinnis, S., Nunes, A., and Qian, Y. (2009), "A Regional Climate Change Assessment Program for North America," *EOS Transactions*, 90, 311.

Murphy, J., Booth, B., Collins, M., Harris, G., Sexton, D., and Webb, M. (2007), "A Methodology for Probabilistic Predictions of Regional Climate Change from Perturbed Physics Ensembles," *Philosophical Transactions of the Royal Society, Series A*, 365, 1993–2028.

Nakicenovic, N., et al. (2000), *Special Report on Emissions Scenarios: A Special Report of Working Group III of the Intergovernmental Panel on Climate Change*, Cambridge: Cambridge University Press.

Rue, H., and Held, L. (2005), *Gaussian Markov Random Fields: Theory and Application*, Boca Raton: Chapman & Hall/CRC Press.

Sain, S., Nychka, D., and Mearns, L. (2011), "Functional ANOVA and Regional Climate Experiments: A Statistical Analysis of Dynamic Downscaling," *Environmetrics*. doi:*10.1002/env.1068*.

Sain, S. R., Furrer, R., and Cressie, N. (2011), "A Spatial Analysis of Multivariate Output From Regional Climate Models," *Annals of Applied Statistics*, 5, 150–175. doi:*10.1214/10-AOAS369*.

Smith, R. L., Tebaldi, C., Nychka, D., and Mearns, L. O. (2009), "Bayesian Modeling of Uncertainty in Ensembles of Climate Models," *Journal of the American Statistical Association*, 104, 97–116. doi:*10.1198/jasa.2009.0007*.

Solomon, S., Qin, D., Manning, M., Chen, Z., Marquis, M., Averyt, K. B., Tignor, M., and Miller, H. L. (eds.) (2007), *Climate Change 2007: The Physical Science Basis: Working Group I Contribution to the Fourth Assessment Report of the IPCC*, Cambridge: Cambridge University Press.

Tebaldi, C., and Knutti, R. (2007), "The Use of the Multimodel Ensemble in Probabilistic Climate Projections," *Philosophical Transactions of the Royal Society A*, 365 (1857), 2053–2075. doi:*10.1098/rsta.2007.2076*.

Tebaldi, C., and Sansó, B. (2009), "Joint Projections of Temperature and Precipitation Change from Multiple Climate Models: A Hierarchical Bayes Approach," *Journal of the Royal Statistical Society, Series A*, 172, 83–106.

Tebaldi, C., Smith, R. L., Nychka, D., and Mearns, L. O. (2005), "Quantifying Uncertainty in Projections of Regional Climate Change: A Bayesian Approach to the Analysis of Multimodel Ensembles," *Journal of Climate*, 18, 1524–1540.